eXPRESS Polymer Letters Vol.6, No.12 (2012) 954–964
Available online at www.expresspolymlett.com
DOI: 10.3144/expresspolymlett.2012.101

High performance polyethylene nanocomposite fibers

M. D'Amato, A. Dorigato, L. Fambri, A. Pegoretti*

University of Trento, Department of Materials Engineering and Industrial Technologies and INSTM Research Unit, Via Mesiano 77, 38123 Trento, Italy

Received 16 April 2012; accepted in revised form 2 July 2012

Abstract. A high density polyethylene (HDPE) matrix was melt compounded with 2 vol% of dimethyldichlorosilane treated fumed silica nanoparticles. Nanocomposite fibers were prepared by melt spinning through a co-rotating twin screw extruder and drawing at 125°C in air. Thermo-mechanical and morphological properties of the resulting fibers were then investigated. The introduction of nanosilica improved the drawability of the fibers, allowing the achievement of higher draw ratios with respect to the neat matrix. The elastic modulus and creep stability of the fibers were remarkably improved upon nanofiller addition, with a retention of the pristine tensile properties at break. Transmission electronic microscope (TEM) images evidenced that the original morphology of the silica aggregates was disrupted by the applied drawing.

Keywords: *nanocomposites, high density polyethylene, fibers, silica*

1. Introduction

In the last two decades it has been widely proven that the mechanical properties (such as elastic modulus, strength, fracture toughness, creep stability and fatigue resistance) of various polymeric matrices can be remarkably improved through the addition of very small amounts (less than 5 wt%) of nanostructured fillers [1]. In particular, a substantial improvement of the thermo-mechanical properties of polymer matrices has been reached by the introduction of high aspect ratio fillers, such as carbon nanotubes [2–4] and layered silicates [5–10]. Compared to the extended literature concerning these kinds of nanofillers, relatively few attention has been devoted to nanocomposites filled with metal oxide nanoparticles, such as fumed titania [11, 12] and fumed silica [13–15]. For instance, Chaichana *et al.* [16] developed a novel route to synthesize linear low density polyethylene (LLDPE)/nanosilica systems via *in situ* polymerization with a zirconocene/methyl alumoxane (MAO) catalyst, in order to study the effect of particle size on the catalytic properties of the resulting materials. The effect of silica and zirconia nanoparticles on the microstructure of LLDPE nanocomposites synthesized via *in situ* polymerization with zirconocene was investigated by Jongsomjit *et al.* [17], while Wang *et al.* [18] analyzed the dispersion behaviour of titania (TiO_2) nanoparticles in polyolefin nanocomposites.

In recent years an extended investigation was carried out by this research group on the viscoelastic and the fracture behavior of polyolefin based nanocomposites [19–23]. It was found that the addition of small quantities of fumed silica nanoparticles could substantially improve both the failure properties and the creep stability of the investigated matrices. High-density polyethylene (HDPE) is a widely applied thermoplastic polymer, characterized by good tensile properties, flexibility, low cost and chemical resistance. For this combination of properties it is used in several industrial applications, such as piping systems, bags, bottles, ropes and fibers. The production of high stiffness and high strength

*Corresponding author, e-mail: andrea.dorigato@ing.unitn.it

polyethylene fibers has been one of the challenges for polymer scientist and engineers for a very long time [24, 25]. One possible way to obtain high performance polyethylene fibers is through melt spinning and subsequent drawing. However, the applications of such fibers have been often limited by their relatively poor creep resistance and low shear modulus and strength. Even if theoretical stress at break values of polyethylene fibers are very high (close to 25 GPa) [26], the strength of highly drawn PE is generally limited to around 1.0–1.3 GPa [27, 28]. Very recently, Toyobo company developed an innovative high strength melt spinning polyethylene fiber (Tsunooga®) with superior lightness and cut resistance, with tenacity of 14 cN/tex and specific gravity of 0.97 g/cm^3, corresponding to a tensile strength of 1.36 GPa. Moreover, it was recently found that the introduction of small amounts of layered silicates in polyethylene matrices may lead to substantial improvements of the mechanical performances of the resulting fibers, in terms of elastic modulus and tensile properties at break [29]. Many efforts were devoted by La Mantia and his group in the investigation of the influence of the elongational flow on the morphology of PE/clay nanocomposite drawn fibers [30]. It was demonstrated how an increase of the elastic modulus and of tensile strength with respect to the neat matrix could be obtained when elevated draw ratios are reached. The observed increase of the mechanical properties was related to the exfoliation and orientation of nanoplatelets induced by the applied flow. Mezghani *et al.* studied the effect of carbon nanotubes (CNT) added to linear low-density polyethylene nanocomposite fibers, prepared by melt extrusion and subsequent cold drawing [31]. The observed improvements of the tensile strength and fiber ductility were attributed to the alignment and distribution of CNT in the organic matrix. Ruan *et al.* [32] reported the use of multiwalled carbon nanotubes (MWCNT) to reinforce and toughen gel-spun ultra high molecular weight polyethylene (UHMWPE) fibers, evidencing some beneficial effects on the tensile strength and strain at break values. The authors explained how nanofiller alignment along the tensile draw direction induced a stronger interfacial load transfer at the interface, enhancing therefore the stiffness and tensile strength of the composite fibers.

Regarding the use of silica nanoparticles to reinforce polyethylene fibers, only Zhang *et al.* [33] recently reported on the morphological, adhesive and mechanical properties of UHMWPE/silica nanocomposite fibers. Nano-silica was able to promote lower crystal sizes and higher crystallinity with respect to the neat fibers, with a remarkable enhancement of their mechanical properties and beneficial effects on the interfacial adhesion with an epoxy matrix. In a preliminary work of this group [23], a high density polyethylene matrix was melt compounded with various untreated (hydrophilic) and surface treated (hydrophobic) fumed silica nanoparticles, having different surface areas. The homogeneous distribution of fumed silica aggregates at low filler contents led to remarkable improvements of the thermal stability and of the ultimate tensile mechanical properties, both under quasi-static and impact conditions. On the basis of these preliminary indications, in the present paper organo-treated fumed silica nanoparticles (Aerosil® R974) were added at a given filler amount (2 vol%) to a HDPE matrix to prepare highly drawn nanocomposite fibers. The influence of fumed silica nanoparticles on the thermo–mechanical behavior of the resulting fibers, with particular attention to their quasi-static tensile and creep behaviour, was investigated.

2. Experimental section

2.1. Materials

High density polyethylene Eltex® A4009 (melt flow rate at 190°C and 2.16 kg = 0.8 dg·min^{-1}, density at 23°C = 0.96 g·cm^{-3}) was supplied in the form of fine powder by BP Solvay (Bruxelles, Belgium). According to the producer's datasheet, the supplied powder has a granulometric distribution comprised between 30 and 1500 μm. Fumed silica nanoparticles Aerosil® R974 were kindly supplied by Evonik (Essen, Germany). Aerosil® R974 is an hydrophobic silica (surface treated with dimethyldichlorosilane) with a specific surface area of 170 m^2·g^{-1} and a bulk density of 1.99 g·cm^{-3} at 23°C. According to the producer's information, this nanofiller is composed by equiaxic nanoparticles with a mean size of 12 nm fused together during the manufacturing operations, forming aggregates of completely amorphous nanoparticles having a mean diameter between 50 and 100 nm. The aggregates are organized in physical

agglomerates that can be partially destroyed during the mixing operations.

Fumed silica nanoparticles were mechanically mixed with HDPE powder at a constant concentration of 2 vol% through a Dispermat F1 mixer, operating at 500 rpm for 5 minutes. The mixture was then melt-compounded in a Thermo-Haake Polylab Rheomix PTW 16p co-rotating intermeshing twin-screw extruder (screw diameter = 16 mm, *L*/*D* ratio = 25, rod die diameter = 1.65 mm). A constant screws speed of 3 rpm was set, while the temperature profile, from hopper to rod die, was as follows: 130, 200, 210, 220 and 220°C. The spun fibers were cooled in water at room temperature and collected on a glass drum (40 mm diameter) rotating at 67 rpm. This speed was kept as low as possible, in order to reduce orientation and drawing of the fibers immediately after the extrusion. In this way filaments having a mean diameter of about 500 μm were produced and were subsequently drawn in air at 125°C at various collecting rate. The differently drawn fibers were distinguished in dependence on the draw ratio (*DR*), that is defined as the ratio between the initial (A_i) and the final cross sectional area (A_f) of the fibers, according to Equation (1):

$$DR = \frac{A_i}{A_f} = \left(\frac{D_i}{D_f}\right)^2 \tag{1}$$

where D_i and D_f indicate the equivalent diameter of the fibers before and after the drawing process, respectively. Neat HDPE fibers were drawn in a stable way up to *DR* values of 45 (diameter = 75 μm), while nanofilled fibers showed an improved drawability, and draw ratios up to 54 (diameter = 68 μm) were reached in a stable manner. The diameter of each fiber was measured by using an optical microscope connected to an image processing software (ImageJ®). Moreover, a draw ratio up to 100 was reached on short segments of nanocomposite fibers in an unstable condition.

2.2. Experimental techniques

Differential scanning calorimetry (DSC) tests were performed by a Mettler DSC30 calorimeter (Schwerzenbach, Switzerland). Samples of about 15 mg were sealed in aluminum pan of 160 microliter and were heated from 0°C up to 200°C at 10°C·min^{-1} flushing nitrogen at 100 mL·min^{-1} and then cooled to 0°C at the same rate. A second heating stage up to 200°C was then carried out. Melting temperature (T_m) and crystalline content (X_c) of the fibers were evaluated. As previously shown in the representative DSC thermograms of compounded HDPE plates and reported in a preliminary work on these nanocomposite systems [23], the melting temperature (T_m) was taken as the peak temperature of the endothermic signal in the DSC plots. Crystallinity (X_c) values were computed by integrating the melting endothermic peaks (ΔH) and considering a reference value of 293 J·g^{-1} for the fully crystalline polyethylene (ΔH_0) [26], i.e. (Equation (2)):

$$X_c = \frac{\Delta H}{\Delta H_0 \cdot W_{HDPE}} \cdot 100 \tag{2}$$

where W_{HDPE} is the weight fraction of HDPE in the composites. A single specimen of fiber at selected equivalent draw ratio of both virgin and nanofilled HDPE was tested.

Dynamical mechanical thermal analysis (DMTA) tests were conducted by a Polymer Laboratories MKII machine in tensile configuration. The tested fibers were folded in an aluminum foil in the grip zone, in order to prevent the slippage of the specimens during the application of the dynamic displacement, and a gage length of 15 mm was set for all the specimens. Mono-frequency tests were performed from –135 to 60°C at a heating rate of 3°C·min^{-1} and a frequency of 5 Hz. A peak to peak displacement of 64 μm was imposed to all the tested specimens, and a pre-stress ranging between 1 and 40 MPa was applied proportionally to the *DR*. Moreover, on neat and nanofilled fibers drawn at a ratio of 45 multi-frequency tests were conducted at 0.3, 1, 3, 5, 10 Hz, in a temperature range from –40 to 60°C at a heating rate of 0.5°C·min^{-1}. A pre-stress of 40 MPa and a peak to peak displacement of 32 μm was applied. According to a frequency-temperature superposition principle [34], storage modulus master curves at the reference temperature of 30°C were generated.

Quasi-static tensile mechanical properties of the fibers were performed by an Instron 4502 tensile testing machine, equipped with a 100 N load cell. According to ASTM C1557 standard, single filaments were cut from the bobbin and glued on paper mounting tabs, with a gage length of 30 mm. Before testing, each specimen was preliminary observed with an Ortholux II POL-BK optical microscope at

different magnifications, in order to determine its diameter. At least five specimens were tested for each sample at a cross-head speed of 50 mm·min^{-1}. Creep response of the fibers at room temperature was tested through the same tensile testing machine, equipped with a load cell of 10 N. Both pure and nanofilled fibers were tested at a constant stress equal to 10% of their quasi-static tensile stress at break. The creep compliance $D(t)$ was computed as the ratio between the deformation and the constant applied stress, and it was monitored over a time interval of 3600 s. Fibers drawn at a draw ratio of 45 were also tested under various creep stresses ranging from 5 to 25% of their tensile stress at break.

In order to have some insight on the microstructural behaviour of the prepared materials, ultramicrotomed cross sections of nanocomposite fibers undrawn (DR = 1) and at the maximum draw ratio (DR = 100) were observed by a Tecnai G2 transmission electron microscope (TEM), supplied by FEI Company (Hillsboro, Oregon, USA), operating at cryogenic temperature (lower than –70°C).

3. Results and discussion

3.1. DSC and DMTA results

In Figure 1a and in Figure 1b DSC thermograms of neat and nanofilled fibers at different DRs are respectively reported, while the most important results obtained from these tests are summarized in Table 1. As it commonly happens in semicrystalline polymers stretched above their glass transition temperature [35, 36], the melting temperature (T_m) increases with the draw ratio. Above a draw ratio of 25, T_m does not increase anymore and tends to level off at a value of about 142°C. At the same time, the crystallinity content increases with the draw ratio up to values in the range of 75–80%. Accordingly to literature [37], it can be hypothesized that the applied drawing induces an ordering of the crystalline phase along the strain direction. Comparing

Table 1. Melting temperature and crystallinity of neat and nanocomposite HDPE fibers from DSC tests (first heating stage)

	T_m [°C]		X_c [%]	
Draw ratio	**HDPE**	**HDPE-2% AR974**	**HDPE**	**HDPE-2% AR974**
1	134.6	131.0	53.5	50.5
7	136.5	138.6	59.3	67.3
25	141.9	142.5	74.0	77.6
40	141.4	142.3	79.9	78.4

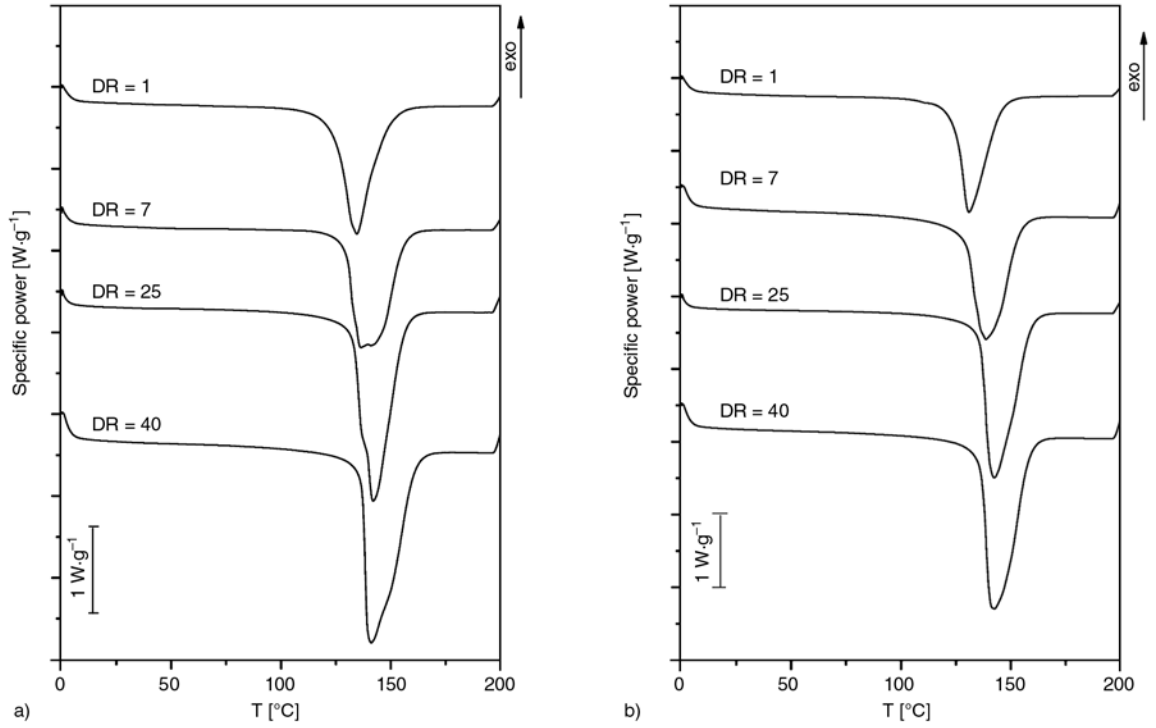

Figure 1. DSC thermograms of (a) neat HDPE and (b) nanocomposite fibers at different DR values (first heating stage)

the crystallinity degree and the melting temperature of pure and nanofilled fibers, it emerges that the introduction of fumed silica nanoparticles plays only a marginal effect on the crystallization behavior of the HDPE. Cooling thermograms evidenced that crystallization temperature of molten fiber range is between 116 and 111°C, directly proportional to the *DR* of the fiber, but in the same it was found independent on the composition. Also the DSC thermograms collected during the second heating stage (here omitted for the sake of brevity) evidenced an independency of both T_m and X_c from the presence of nanosilica. Comparing these results with the literature references, it is difficult to have a clear picture of the effects of nanofillers on the crystallization behaviour of polyethylene fibers. In fact, Zhang *et al.* [33] found an increase of the fiber crystallinity promoted by the addition of surface treated nanosilica in UHMWPE. Also Ruan *et al.* [32] reported that the addition of MWCNT at a concentration of 5 wt% had a nucleating effects on polyethylene crystals, particularly in the highly aligned fibers, but the crystallinity of the composite fibers was slightly lower than that of the pristine fibers. On the other hand, La Mantia *et al.* [30] found that organomodified layered silicates did not have any effect on the crystallization properties of LLDPE fibers and hypothesized that the orientation in both crystalline and amorphous phases were similar for filled and unfilled fibers. According to our previous works on polyethylene based nanocomposites [20, 21, 23], we can hypothesize that the limited influence played by fumed silica nanoparticles on the crystallization properties of our HDPE matrix could be probably ascribed to their dispersion state. However, further investigations are needed to reach a deeper comprehension on the role played by nanosilica on the crystallization behaviour of polyethylene.

It is important to note that the maximum draw ratio reached on nanofilled fibers during the hot stretching and continuous collecting process (*DR* = 54) is significantly higher than that achievable with neat fibers (*DR* = 45). This means that the presence of fumed silica nanoparticles improves fibers drawability. Storage modulus (*E′*) curves of neat polyethylene and nanocomposite fibers obtained in DMTA tests at a frequency of 5 Hz are reported in Figure 2. As expected, the molecular orientation induced by

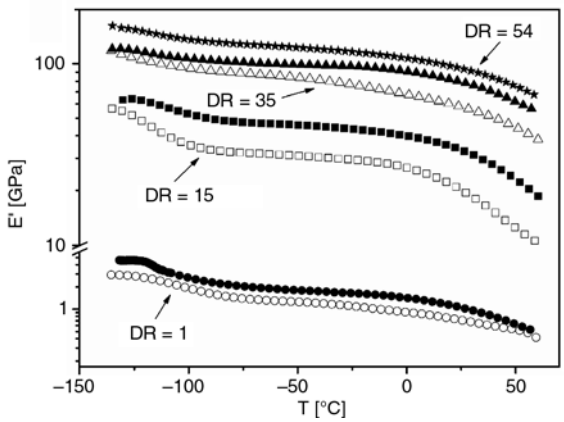

Figure 2. Storage modulus (*E′*) of neat HDPE fibers (open symbols) and nanocomposite fibers (filled symbols) at various draw ratios as determined in DMTA tests at a frequency of 5 Hz

stretching results in a noticeable increase of *E′* values over the whole range of investigated temperatures. The presence of nanosilica produces a remarkable stiffening effect on the resulting fibers. In fact, for any given draw ratio, nanocomposite fibers exhibit higher storage modulus values with respect to the neat ones. It is widely reported in literature how the increase of the elastic properties of the drawn fibers can be due both to the crystallinity increase induced by the molecular orientation and to possible changes in the crystal size/morphology promoted by the cold drawing process [38]. Also nanoparticles can alter crystallization behaviour of the nanofilled fibers [30, 32, 33]. In our case, DSC tests on the nanofilled fibers excluded any effect on the overall crystallinity degree due to the nanofiller introduction, but it is possible to hypothesize that crystal size could be altered by the presence of silica aggregates within the matrix. However, it is only an hypothesis, and only a detailed study on the crystallization properties of nanofilled fibers could provide a satisfactory answer to this point. In the future, further efforts will be made to better understand the crystallization behaviour of the investigated systems. In order to evaluate the dynamic behaviour over an extended frequency range, multi-frequency DMTA tests were also performed on high drawn neat and nanofilled fibers (*DR* = 45). Figure 3 reports the resulting master curves obtained on the basis of a frequency-temperature superposition principle at a reference temperature of 30°C. Over the entire frequency range, storage modulus values of nanofilled fibers are higher than those of unfilled fibers. From

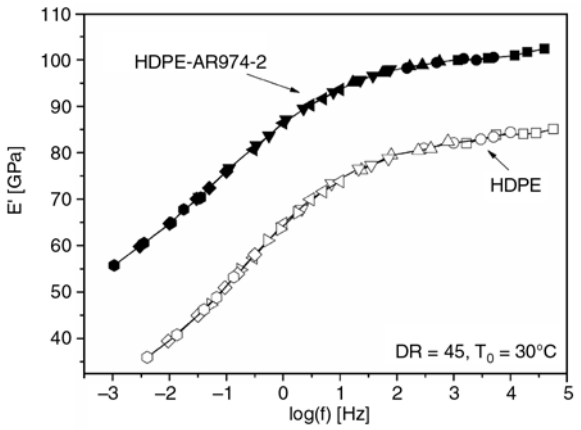

Figure 3. Storage modulus (E') master curves of neat HDPE fibers (open symbols) and nanocomposite (filled symbols) fibers at DR = 45 from DMTA multi-frequency tests (T_0 = 30°C)

the correspondent plot of the shift factors as a function of temperature (not reported for the sake of brevity) an Arrhenius type trend can be observed [34], characterized by an activation energy of the viscoelastic process of 147+2 kJ·mol^{-1} for the neat specimens and 167+6 kJ·mol^{-1} for nanofilled HDPE fibers.

3.2. Quasi-static and creep tensile properties

Elastic modulus (E) values of the tested fibers as a function of the draw ratio are summarized in Figure 4a, while stress (σ_B) and strain (ε_B) at break values are reported in Figure 4b and Figure 4c, respectively. According to DMTA results, it is evident that the presence of fumed silica nanoparticles produces a significant increase of the elastic modulus, especially at elevated draw ratios. Furthermore, the possibility of reaching higher draw ratios with the nanosilica introduction allows us to prepare fibers possessing higher elastic moduli (about 55 GPa for a DR of 54). Interestingly, the increase of the fibers stiffness can be obtained without impairing their tensile properties at break. In fact, both stress and strain at break values do not appear to be influenced by the presence of nanofiller. The better drawability of nanofilled fibers offers the possibility to reach higher stress at break values (about 1.65 GPa for a DR of 54).

Figure 5a displays creep compliance curves for neat and nanocomposite polyethylene fibers drawn at various DRs and loaded at a stress level equal to 10% of their stress at break values. Even if at DR = 1 the creep compliance of the nanocomposite fibers is

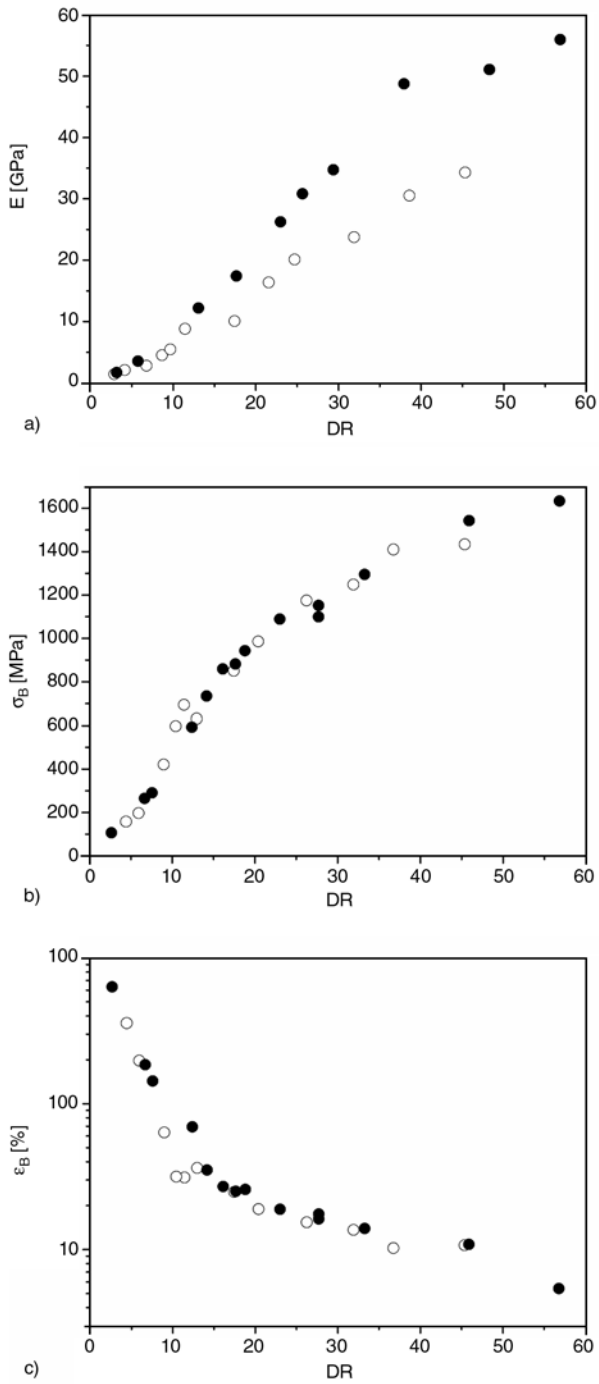

Figure 4. Mechanical properties of neat HDPE fibers (open symbols) and nanocomposite fibers (filled symbols) from quasi-static tensile tests: (a) Elastic modulus, (b) Stress at break, (c) Strain at break

practically equal to that of the unfilled ones, an interesting improvement of the creep stability due to the nanofiller introduction can be detected as the draw ratio increases. This trend can be clearly evidenced in the plot of creep compliance values at 3600 s as a function of the draw ratio (Figure 5b).

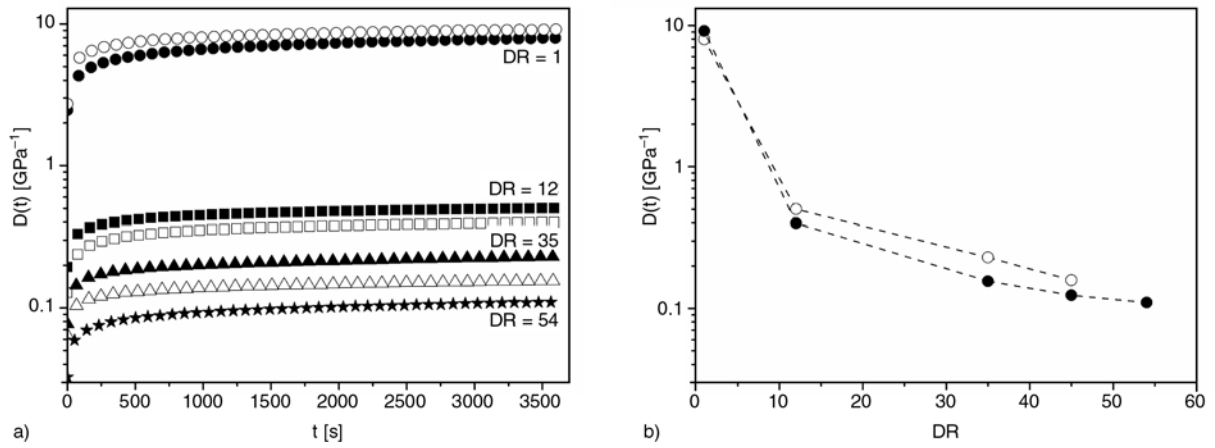

Figure 5. Creep tests on neat HDPE fibers (open symbols) and nanocomposite fibers (filled symbols) at σ_0 = 10% of σ_B: (a) creep compliance curves at various draw ratios, (b) creep compliance values at 3600 s as a function of the draw ratio

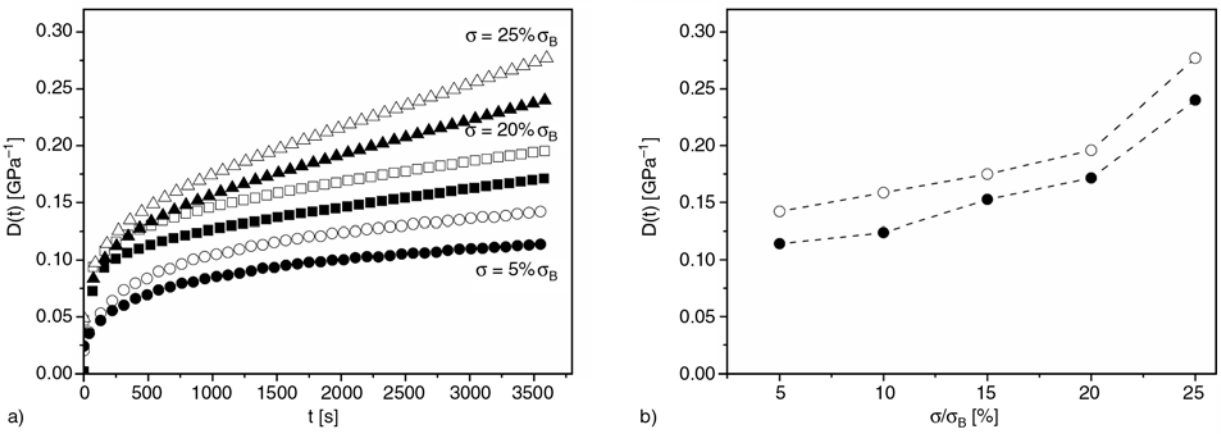

Figure 6. Creep tests on neat HDPE fibers (open symbols) and nanocomposite fibers (filled symbols) at *DR* = 45: (a) creep compliance curves at various stress levels, (b) creep compliance after 3600 s as a function of the normalized stress

In order to evaluate the effect of the applied stress on the creep behaviour of the tested fibers, creep compliance curves of neat and nanocomposite fibers processed at *DR* = 45 are reported in Figure 6a for various stress levels. Once again, the presence of the nanofiller produces an interesting decrease of the creep compliance values with respect to the neat HDPE fibers for all the investigated stress levels. Furthermore, if creep compliance values at 3600 s are compared for various stress levels (Figure 6b) it emerges that, in absolute value, the stabilizing effect provided by nanosilica introduction is not substantially influenced by the stress level.

3.3. Microstructure

Concerning the polymer microstructure in the fibers, considering that DSC evidenced how both melting temperature and crystallinity degree are about the same for both materials (see Table 1), it is reasonable to hypothesize that the orientation of HDPE macromolecules both in crystalline and in amorphous phases is similar for neat and nanocomposite fibers. These results are in good agreement with the conclusions reported by La Mantia *et al.* [30]. Therefore, the experienced increase of the mechanical properties due to nanosilica introduction cannot be attributed to different chain orientation in the tested materials. In our previous work on the fracture behavior of LLDPE/fumed silica nanocomposites [39], the enhancement of mechanical properties observed for nanocomposites was explained as an effect of the progressive alignment of nanofiller aggregates along the strain direction. In order to support this hypothesis, TEM images of the ultramicrotomed cross sections of nanofilled fibers at *DR* = 1 (undrawn fibers) and at *DR* = 100 are respectively reported in Figure 7a and in Figure 7b. Undrawn fibers are characterized by the presence of fumed

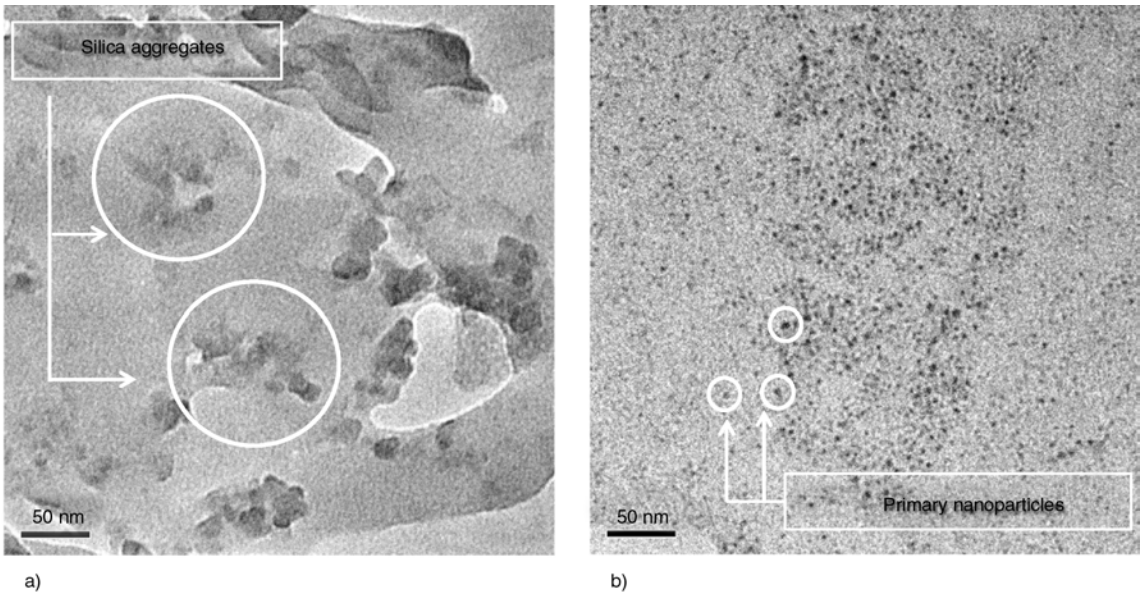

Figure 7. TEM images of ultra-microtomed cross-sections of (a) undrawn (*DR* = 1) and (b) highly drawn (*DR* = 100) nanocomposite fibers

silica nanoparticles uniformly dispersed in the matrix forming isodimensional clusters of aggregated primary nanoparticles having a mean size lower than 100 nm. It is difficult to assess whether the clusters are constituted by aggregation of primary nanoparticles fused together during the manufacturing process or if they are formed by physical agglomeration of aggregates. However, it is evident that agglomerates are relatively small and apparently well dispersed within the matrix. This could justify the retention of the tensile properties at break experienced in quasi-static tests. A similar microstructure was observed for HDPE/fumed silica composites obtained by melt compounding and compression molding [23]. This means that melt spinning process has a negligible effects on the microstructural behaviour of the prepared materials, because chain alignment along the flow direction is not followed by a deformation and/or rupture of silica aggregates. This could explain why at *DR* = 1 the tensile properties of nanofilled fibers are very near to those of the unfilled ones. The microstructure is very different when an elevated draw ratio is applied to the fibers (Figure 7b). In this case the drawing process produces the rupture of silica aggregates and, most probably, their alignment along the cold drawing direction. In the cryofractured sections it is possible to detect the presence of individual primary nanoparticles having a mean size of about 10 nm, in good agreement with the indication reported in the datasheet by the producer. Unfortunately, due to the experimental difficulties in preparing thin sections of the fiber along their axis, no direct evidence of the alignment phenomenon can be experimentally provided. Nevertheless, we recently reported a direct experimental evidence of alignment of streams of nanoparticle along the drawing direction in a similar system consisting of an LLDPE matrix filled with fumed silica nanoparticles [39]. This means that the agglomerates of fumed metal oxides nanoparticles, once exposed to an elongational flow in the solid state, orient themselves along the strain direction. Unlike conventional microfillers, fumed silica aggregates can be deformed and fractured to form long streams of nanoparticles dispersed within the polymer matrix. This process is very similar to the exfoliation process induced by the flow in polymer/clay nanocomposites with a good affinity between the two components [40]. Therefore, the larger enhancement of the elastic modulus observed for the nanofilled samples at elevated filler contents cannot be attributed solely to the orientation of the polyethylene macromolecules. The elongational flow, unlike the shear flow, is able to break and orient the dispersed nanoparticle aggregates even if the viscosity ratio of the two phases is very different, and the dramatic increase of the filler-matrix interfacial area could be thus responsible of the observed increase of the mechanical properties. As explained in Paragraph 3.1, nanofiller introduction

could alter the crystal size/morphology of the oriented matrix, with important consequences on the mechanical behaviour of the resulting material. Therefore, the stiffening effect due to silica nanoparticles experienced in this work can be probably ascribed both to an increase of the filler-matrix interfacial area due to the aggregates elongation, and to possible changes in the crystalline morphology of the matrix. However, these two effects play a synergistic role in polymer processing expecially for fiber production, where the phenomenon of crystallization-induced-orientation affects mechanical properties, and the amorphous phase orientation is also involved.

4. Conclusions

Surface treated fumed silica nanoparticles were melt compounded with a high density polyethylene matrix in order to produce nanocomposite fibers in a double step process of extrusion and drawing. Fibers stiffness was remarkably improved by nanofiller introduction, especially at elevated draw ratios, without affecting tensile properties at break of the pristine fibers. DSC tests evidenced how both the melting temperature and the crystallinity degree of the fibers are not substantially affected by the nanosilica introduction. Also creep tests evidenced a certain reduction of the creep compliance with respect to the neat HDPE fibers over the whole range of investigated draw ratios and applied stresses. TEM images revealed how the experienced improvements of the mechanical properties could be probably related to the strong alignment of silica aggregates along the strain direction and to the consequent increase of the filler-matrix interfacial area. Moreover, the stiffening effect of the nanofiller in drawn fiber is also confirmed from dynamical mechanical analysis, as evidenced from the higher storage modulus in the range of temperature (–40°C/+60°C) and the higher master curve of storage modulus at 30°C in the range of frequency (10^{-3}–10^{5} Hz).

Acknowledgements

A grateful acknowledgement to prof. Z. Zhang of the National Center for Nanoscience and Technology (Beijing, China) for the TEM images of nanocomposite fibers.

References

[1] Hussain F., Hojjati M., Okamoto M., Gorga R. E.: Review article: Polymer-matrix nanocomposites, processing, manufacturing, and application: An overview. Journal of Composite Materials, **40**, 1511–1575 (2006). DOI: 10.1177/0021998306067321

[2] Chrissafis K., Paraskevopoulos K. M., Tsiaoussis I., Bikiaris D.: Comparative study of the effect of different nanoparticles on the mechanical properties, permeability, and thermal degradation mechanism of HDPE. Journal of Applied Polymer Science, **114**, 1606–1618 (2009). DOI: 10.1002/app.30750

[3] Li S., Chen H., Cui D., Li J., Zhang Z., Wang Y., Tang T.: Structure and properties of multi-walled carbon nanotubes/polyethylene nanocomposites synthesized by *in situ* polymerization with supported Cp_2ZrCl_2 catalyst. Polymer Composites, **31**, 507–515 (2010). DOI: 10.1002/pc.20831

[4] Yang B-X., Pramoda K. P., Xu G. Q., Goh S. H.: Mechanical reinforcement of polyethylene using polyethylene-grafted multiwalled carbon nanotubes. Advanced Functional Materials, **17**, 2062–2069 (2007). DOI: 10.1002/adfm.200600599

[5] Dorigato A., Morandi S., Pegoretti A.: Effect of nanoclay addition on the fiber/matrix adhesion in epoxy/glass composites. Journal of Composite Materials, **46**, 1439–1451 (2012). DOI: 10.1177/0021998311420311

[6] Dorigato A., Pegoretti A.: Development and thermomechanical behavior of nanocomposite epoxy adhesives. Polymers for Advanced Technologies, **23**, 660–668 (2012). DOI: 10.1002/pat.1942

[7] Dorigato A., Pegoretti A., Penati A.: Effect of the polymer–filler interaction on the thermo-mechanical response of polyurethane-clay nanocomposites from blocked prepolymer. Journal of Reinforced Plastics and Composites, **30**, 325–335 (2011). DOI: 10.1177/0731684410396599

[8] Lee E. M., Oh Y. S., Ha H. S., Jeong H. M., Kim B. K.: Ultra high molecular weight polyethylene/organoclay hybrid nanocomposites. Journal of Applied Polymer Science, **114**, 1529–1534 (2009). DOI: 10.1002/app.30736

[9] Mandalia T., Bergaya F.: Organo clay mineral–melted polyolefin nanocomposites effect of surfactant/CEC ratio. Journal of Physics and Chemistry of Solids, **67**, 836–845 (2006). DOI: 10.1016/j.jpcs.2005.12.007

[10] Pegoretti A., Dorigato A., Brugnara M., Penati A.: Contact angle measurements as a tool to investigate the filler–matrix interactions in polyurethane–clay nanocomposites from blocked prepolymer. European Polymer Journal, **44**, 1662–71672 (2008). DOI: 10.1016/j.eurpolymj.2008.04.011

[11] Bondioli F., Dorigato A., Fabbri P., Messori M., Pegoretti A.: High-density polyethylene reinforced with submicron titania particles. Polymer Engineering and Science, **48**, 448–457 (2008).
DOI: 10.1002/pen.20973

[12] Bondioli F., Dorigato A., Fabbri P., Messori M., Pegoretti A.: Improving the creep stability of high-density polyethylene with acicular titania nanoparticles. Journal of Applied Polymer Science, **112**, 1045–1055 (2009).
DOI: 10.1002/app.29472

[13] Kontou E., Niaounakis M.: Thermo-mechanical properties of LLDPE/SiO_2 nanocomposites. Polymer, **47**, 1267–1280 (2006).
DOI: 10.1016/j.polymer.2005.12.039

[14] Yang F., Nelson G. L.: PMMA/silica nanocomposite studies: Synthesis and properties. Journal of Applied Polymer Science, **91**, 3844–3850 (2004).
DOI: 10.1002/app.13573

[15] Zhang M. Q., Rong M. Z., Zhang H. B., Friedrich K.: Mechanical properties of low nano-silica filled high density polyethylene composites. Polymer Engineering and Science, **43**, 490–500 (2003).
DOI: 10.1002/pen.10040

[16] Chaichana E., Jongsomjit B., Praserthdam P.: Effect of nano-SiO_2 particle size on the formation of LLDPE/SiO_2 nanocomposite synthesized via the *in situ* polymerization with metallocene catalyst. Chemical Engineering Science, **62**, 899–905 (2007).
DOI: 10.1016/j.ces.2006.10.005

[17] Jongsomjit B., Panpranot J., Praserthdam P.: Effect of nanoscale SiO_2 and ZrO_2 as the fillers on the microstructure of LLDPE nanocomposites synthesized via *in situ* polymerization with zirconocene. Materials Letters, **61**, 1376–1379 (2007).
DOI: 10.1016/j.matlet.2006.07.034

[18] Wang Z., Li G., Xie G., Zhang Z.: Dispersion behavior of TiO_2 nanoparticles in LLDPE/LDPE/TiO_2 nanocomposites. Macromolecular Chemistry and Physics, **206**, 258–262 (2005).
DOI: 10.1002/macp.200400309

[19] Dorigato A., Pegoretti A.: Tensile creep behaviour of polymethylpentene–silica nanocomposites. Polymer International, **59**, 719–724 (2010).
DOI: 10.1002/pi.2769

[20] Dorigato A., Pegoretti A., Kolařík J.: Nonlinear tensile creep of linear low density polyethylene/fumed silica nanocomposites: Time-strain superposition and creep prediction. Polymer Composites, **31**, 1947–1955 (2010).
DOI: 10.1002/pc.20993

[21] Dorigato A., Pegoretti A., Penati A.: Linear low-density polyethylene/silica micro- and nanocomposites: Dynamic rheological measurements and modelling. Express Polymer Letters, **4**, 115–129 (2010).
DOI: 10.3144/expresspolymlett.2010.16

[22] Dorigato A., Pegoretti A., Fambri L., Slouf M., Kolarik J.: Cycloolefin copolymer/fumed silica nanocomposites. Journal of Applied Polymer Science, **119**, 3393–3402 (2011).
DOI: 10.1002/app.32988

[23] Dorigato A., D'Amato M., Pegoretti A.: Thermo-mechanical properties of high density polyethylene – fumed silica nanocomposites: Effect of filler surface area and treatment. Journal of Polymer Research, **19**, 9889–9899 (2012).
DOI: 10.1007/s10965-012-9889-2

[24] Pennings A. J., Smook J., De Boer J., Gogolewski S., van Hutten P. F.: Process of preparation and properties of ultra-high strength polyethylene fibers. Pure and Applied Chemistry, **55**, 777–798 (1983).

[25] Smith P., Lemstra P. J., Kalb B., Pennings A. J.: Ultra-high-strength polyethylene filaments by solution spinning and hot drawing. Polymer Bulletin, **1**, 733–736 (1979).
DOI: 10.1007/BF00256272

[26] Van Krevelen D. W.: Properties of polymers. Elsevier. Amsterdam (1990).

[27] Smith P., Lemstra P. J., Pijpers J. P. L.: Tensile strength of highly oriented polyethylene. II. Effect of molecular weight distribution. Journal of Polymer Science Part B: Polymer Physics, **20**, 2229–2241 (1982).
DOI: 10.1002/pol.1982.180201206

[28] Salem D. R.: Structure formation in polymeric fibers. Hanser, Munich (2005).

[29] Chantrasakul S., Amornsakchai T.: High strength polyethylene fibers from high density polyethylene/organoclay composites. Polymer Engineering and Science, **47**, 943–950 (2007).
DOI: 10.1002/pen.20778

[30] La Mantia F. P., Dintcheva N. T., Scaffaro R., Marino R.: Morphology and properties of polyethylene/clay nanocomposite drawn fibers. Macromolecular Materials and Engineering, **293**, 83–91 (2008).
DOI: 10.1002/mame.200700204

[31] Mezghani K., Farooqui M., Furquan S., Atieh M.: Influence of carbon nanotube (CNT) on the mechanical properties of LLDPE/CNT nanocomposite fibers. Materials Letters, **65**, 3633–3635 (2011).
DOI: 10.1016/j.matlet.2011.08.002

[32] Ruan S., Gao P., Yu T. X.: Ultra-strong gel-spun UHMWPE fibers reinforced using multiwalled carbon nanotubes. Polymer, **47**, 1604–1611 (2006).
DOI: 10.1016/j.polymer.2006.01.020

[33] Zhang Y., Yu J., Zhou C., Chen L., Hu Z.: Preparation, morphology, and adhesive and mechanical properties of ultrahigh-molecular-weight polyethylene/SiO_2 nanocomposite fibers. Polymer Composites, **31**, 684–690 (2010).
DOI: 10.1002/pc.20847

[34] Riande E., Calleja R. D., Prolongo M., Masegosa R.: Polymer viscoelasticity, stress and strain in practice. Marcel Dekker, New York (2000).

[35] Anandakumaran K., Roy S. K., St. John Manley R.: Drawing-induced changes in the properties of polyethylene fibers prepared by gelation/crystallization. Macromolecules, **21**, 1746–1751 (1988).
DOI: 10.1021/ma00184a036

[36] Selikhova V. I., Ozerina L. A., Ozerin A. N., Bakeyev N. F.: Special melting behaviour of highly oriented polyethylene. Polymer Science U.S.S.R., **28**, 378–385 (1986).
DOI: 10.1016/0032-3950(86)90094-8

[37] Capaccio G., Crompton T. A., Ward I. M.: Ultra-high modulus polyethylene by high temperature drawing. Polymer, **17**, 644–645 (1976).
DOI: 10.1016/0032-3861(76)90288-3

[38] Humphreys J., Ward I. M., Nix E. L., McGrath J. C., Emi T.: A study of the drawing behavior of polyvinylidene fluoride. Journal of Applied Polymer Science, **30**, 4069–4079 (1985).
DOI: 10.1002/app.1985.070301010

[39] Dorigato A., Pegoretti A.: Fracture behaviour of linear low density polyethylene – fumed silica nanocomposites. Engineering Fracture Mechanics, **79**, 213–224 (2012).
DOI: 10.1016/j.engfracmech.2011.10.014

[40] Tokihisa M., Yakemoto K., Sakai T., Utracki L. A., Sepehr M., Li J., Simard Y.: Extensional flow mixer for polymer nanocomposites. Polymer Engineering and Science, **46**, 1040–1050 (2006).
DOI: 10.1002/pen.20542